Nonholomorphic soft-term contributions to the Higgs-boson masses in the Feynman diagrammatic approach

M. Rehman[1,*] and S. Heinemeyer[2,†]

[1]Department of Physics, Comsats University Islamabad, 44000 Islamabad, Pakistan
[2]Instituto de Física Teórica, (UAM/CSIC), Universidad Autónoma de Madrid, Cantoblanco, 28049 Madrid, Spain

(Received 4 January 2023; accepted 8 May 2023; published 23 May 2023)

We study the effects of nonholomorphic soft supersymmetry-breaking terms added to the minimal supersymmetric Standard Model on the Higgs-boson masses. The calculation of the nonholomorphic contributions is performed at the one-loop level in the Feynman diagrammatic approach. After generating a FeynArts model file with the help of SARAH, we calculate the renormalized Higgs-boson self-energies at the one-loop level using the FeynArts/FormCalc setup. The results obtained from FeynArts/FormCalc are fed to FeynHiggs to estimate the contributions to the neutral CP-even Higgs-boson masses, $M_{h,H}$, as well as to the charged Higgs-boson mass, $M_{H^\pm}$. For the specific set of parameter points that we choose for this study, the nonholomorphic soft-term contributions to the light CP-even Higgs-boson mass, M_h, contrary to claims in the literature, turn out to be very small. For the heavy CP-even Higgs-boson mass, M_H, as well as for the charged Higgs-boson mass, $M_{H^\pm}$, the contributions can be substantially larger for some parts of parameter space.

DOI: 10.1103/PhysRevD.107.095033

I. INTRODUCTION

After the Higgs-boson discovery at the Large Hadron Collider (LHC) [1,2], much attention has been devoted to measuring the mass and other properties of the Higgs boson as precisely as possible. These properties, within the current experimental and theoretical uncertainties, are in agreement with the Standard Model (SM) predictions [3]. Consequently, any model beyond the SM (BSM) should contain a state matching the LHC mass and rate measurements. The requirement imposes strong constraints on any BSM parameter space. On the other hand, the absence of discovery of any (additional) BSM particles also imposes severe constraints on the new physics parameters. Due to these reasons, the minimal supersymmetric Standard Model (MSSM) [4], which is probably the best and most studied extension of the SM, is also facing severe constraints on its parameter space. For example, the present value of the Higgs-boson mass $M_H^{\rm obs} = 125.38 \pm 0.14$ GeV [5] requires the supersymmetry (SUSY) partners of the top quark, the scalar tops, to be either in the multi-TeV range or that some relations among their parameters are fulfilled. One way to deal with this problem would be to look for extra sources for the radiative corrections while keeping the sfermion masses light. Left-right mixing and flavor mixing in the sfermions can serve the purpose to some extent [6,7]. See Ref. [8] for a recent review on SUSY Higgs-boson mass calculations.

In this paper, we will take a different route. In the MSSM, the superpotential and soft SUSY-breaking terms are generally considered holomorphic functions. While the superpotential must be holomorphic, the soft SUSY-breaking terms can be nonholomorphic (NH) in nature [9,10]. For further reference, we will call this setup the Nonholomorphic supersymmetric Standard Model (NHSSM). In general, the NH soft SUSY-breaking terms can contribute to the radiative corrections to the Higgs-boson masses. The question arises whether this additional freedom in the form of NH soft SUSY-breaking terms has the potential to increase the value of the light CP-even Higgs-boson mass in a relevant way. Some of the previous analyses of the NH effects particularly to the Higgs boson sector can be found in Refs. [11–16]. More recently in Ref. [17], it was reported that the NH soft SUSY-breaking terms can enhance/decrease the light CP-even Higgs-boson mass M_h by up to 3 GeV. The analyses in this regard focused only on the leading top-stop contributions to the Higgs sector. In Ref. [17] (see also Ref. [18]) the effects of NH soft SUSY-breaking terms on M_h via their effects on the scalar top masses were calculated. The NH terms enter the scalar top sector through left-right mixing parameter X_t. However, the observed effects can be mimicked by a change in the holomorphic soft SUSY-breaking

*m.rehman@comsats.edu.pk
†Sven.Heinemeyer@cern.ch

terms, in particular the trilinear Higgs-stop coupling, A_t; for each choice of A_t' the parameter A_t can be adjusted to yield the same scalar top masses and mixing angle. An observed scalar top mass spectrum thus corresponds to a continuous set of combinations of A_t and A_t' (keeping the other soft SUSY-breaking parameters and μ fixed). An analysis that simply varies A_t', resulting in shifts in the scalar top masses and mixing angle, can thus not be regarded as realistic. On the other hand, the analysis in Ref. [17] neglected the effects of the NH terms entering the Higgs-sfermion couplings. As NH soft SUSY-breaking terms also enter the couplings of the Higgs bosons to the scalar fermions, it is important to consider all possible effects simultaneously, while clearly working out the genuine NH effects.

In this work, we have calculated the effects of NH soft SUSY-breaking term A_t' to the Higgs-boson mass spectra at the one-loop level using the Feynman diagrammatic approach. These newly evaluated one-loop corrections, obtained by FeynArts/FormCalc setup [19–22], were then fed into FeynHiggs [23–30] such that all other known higher-order corrections can be taken over from the MSSM. We ensured that the stop spectrum does not change under the variation of A_t'. This allows us to reliably estimate the effects of the NH soft SUSY-breaking terms to the Higgs-boson masses at the one-loop level.

The paper is organized as follows: First, we present the main features of the NHSSM in Sec. II. The computational setup is given in Sec. III. The numerical results are presented in Sec. IV. Our conclusions can be found in Sec. V.

II. MODEL SETUP

The MSSM is the simplest supersymmetric structure one can build from the SM particle content. The general setup for the soft SUSY-breaking parameters is given by [4]

$$\begin{aligned}-\mathcal{L}_{\text{soft}} &= (m_{\tilde{Q}}^2)_i^j \tilde{q}_L^{\dagger i}\tilde{q}_{Lj} + (m_{\tilde{u}}^2)_j^i \tilde{u}_{Ri}^* \tilde{u}_R^j + (m_{\tilde{d}}^2)_j^i \tilde{d}_{Ri}^* \tilde{d}_R^j \\ &+ (m_{\tilde{L}}^2)_i^j \tilde{l}_L^{\dagger i}\tilde{l}_{Lj} + (m_{\tilde{e}}^2)_j^i \tilde{e}_{Ri}^* \tilde{e}_R^j \\ &+ \tilde{m}_1^2 h_1^\dagger h_1 + \tilde{m}_2^2 h_2^\dagger h_2 + (B\mu h_1 h_2 + \text{H.c.}) \\ &+ \Big(A_d^{ij} h_1 \tilde{d}_{Ri}^* \tilde{q}_{Lj} + A_u^{ij} h_2 \tilde{u}_{Ri}^* \tilde{q}_{Lj} + A_l^{ij} h_1 \tilde{e}_{Ri}^* \tilde{l}_{Lj} \\ &+ \frac{1}{2} M_1 \tilde{B}\tilde{B} + \frac{1}{2} M_2 \tilde{W}\tilde{W} + \frac{1}{2} M_3 \tilde{G}\tilde{G} + \text{H.c.} \Big). \end{aligned} \quad (1)$$

Here $m_{\tilde{Q}}^2$ and $m_{\tilde{L}}^2$ are 3×3 matrices in family space (with i, j being the generation indices) for the soft SUSY-breaking masses of the left-handed squark $\tilde{q}_L$ and slepton $\tilde{l}_L$ $SU(2)$ doublets, respectively. $m_{\tilde{u}}^2$, $m_{\tilde{d}}^2$ and $m_{\tilde{e}}^2$ contain the soft masses for right-handed up-type squark $\tilde{u}_R$, down-type squarks $\tilde{d}_R$, and charged slepton $\tilde{e}_R$ $SU(2)$ singlets, respectively. A_u, A_d, and A_l are the 3×3 matrices for the trilinear couplings for up-type squarks, down-type squarks, and charged sleptons, respectively. μ is Higgs mixing parameter, $\tilde{m}_1$, $\tilde{m}_2$, and B are the soft SUSY-breaking parameters of the Higgs sector, where h_1 and h_2 denote the two doublets. In the last line M_1, M_2, and M_3 define the bino, wino, and gluino mass terms, respectively.

The superpotential in the MSSM must be holomorphic, and consequently, the soft SUSY-breaking sector is generally parametrized via holomorphic operators. However, the MSSM can be extended by introducing R-parity-violating and/or nonholomorphic terms in the soft breaking sector [9,10,31]. In its simplest form the following terms can be introduced in the soft SUSY-breaking sector of the MSSM,

$$\begin{aligned}-\mathcal{L}_{\text{soft}}^{\text{NH}} &= A_d'^{ij} h_2 \tilde{d}_{Ri}^* \tilde{q}_{Lj} + A_u'^{ij} h_1 \tilde{u}_{Ri}^* \tilde{q}_{Lj} + A_l'^{ij} h_2 \tilde{e}_{Ri}^* \tilde{l}_{Lj} \\ &+ \mu' \tilde{h}_1 \tilde{h}_2. \end{aligned} \quad (2)$$

Here μ' is the NH higgsino mass term, whereas A_u', A_d', and A_l' denote the NH trilinear coupling matrices for up-type squarks, down-type squarks, and charged sleptons, respectively. These terms do not necessarily have any relationship with the holomorphic trilinear soft terms given in Eq. (1). One possibility is to assume them to be equal to the holomorphic trilinear couplings as a "boundary condition" at the GUT scale in models such as the constrained MSSM. However, even in that case, renormalization group-equation running effects will result in completely different nonholomorphic trilinear terms [16]. Therefore, it is a sensible approach to consider nonholomorphic trilinear terms independent, but overall of the same order of magnitude as the usual trilinear couplings while comparing the NHSSM predictions with the experimental results.

In the presence of the nonholomorphic trilinear terms, the sfermion mass matrices will be modified as

$$M_{\tilde{f}}^2 = \begin{pmatrix} m_{\tilde{f}LL}^2 & m_{\tilde{f}LR}^2 \\ m_{\tilde{f}LR}^{2\dagger} & m_{\tilde{f}'RR}^2 \end{pmatrix} \quad (3)$$

with

$$\begin{aligned} m_{\tilde{f}LL}^2 &= m_{\tilde{f}}^2 + M_Z^2 \cos 2\beta (I_3^f - Q_f s_W^2) + m_f^2, \\ m_{\tilde{f}'RR}^2 &= m_{\tilde{f}'}^2 + M_Z^2 \cos 2\beta Q_{f'} s_W^2 + m_f^2, \\ m_{\tilde{f}LR}^2 &= m_f X_f; \qquad X_f = A_f - (\mu + A_f')\{\cot\beta; \tan\beta\}, \end{aligned} \quad (4)$$

where I_3^f is the weak isospin of fermions, Q_f is the electromagnetic charge, m_f is the standard fermion mass, f and f' stand for left- and right-handed sfermions (except for sneutrinos), respectively. M_Z and M_W denote the mass of the Z and the W boson, and $s_W = \sqrt{1 - c_W^2}$ with $c_W = M_W/M_Z$. A_f (A_f') is the holomorphic (nonholomorphic) trilinear coupling,[1] μ is the Higgs mixing parameter,

[1]We neglect CP violation throughout the paper.

and $\cot\beta$ is for up-type squarks, and $\tan\beta$ is for down-type squarks and charged sleptons ($\tan\beta := v_2/v_1$, is the ratio of the two vacuum expectation values of the two Higgs doublets.) The NH higgsino mass parameter μ' mentioned in Eq. (2) modifies the neutralino and chargino mass matrices, but it does not enter into the modified sfermion mass matrices. Consequently, it will not be particularly relevant to our present analysis as we focus on the top/stop contributions. It should be noted that because of the different combinations of fields in $\mathcal{L}_{\rm soft}^{\rm NH}$ with respect to $\mathcal{L}_{\rm soft}$, the nonholomorphic trilinear couplings A'_f receive the additional factors of $\tan\beta$ or $\cot\beta$.

As discussed before, the NH trilinear terms also modify the Higgs-sfermion-sfermion couplings. Here we show the couplings of the lightest Higgs boson h to the up-type squarks.

$$C(h,\tilde{u}_i^s,\tilde{u}_j^t) = \frac{-ie\delta_{ij}}{6M_W c_W s_W s_\beta}[3c_W m_{u_i}\{A_{ii}^u c_\alpha + (\mu + A_{ii}'^u)s_\alpha\}U_{s,1}^{\tilde{u},i}U_{t,2}^{\tilde{u},i} + \{6c_\alpha c_W m_{u_i}^2 - M_W M_Z s_{\alpha+\beta}s_\beta(3-4s_W^2)\}U_{s,1}^{\tilde{u},i}U_{t,1}^{\tilde{u},i}$$
$$+ \{6c_\alpha c_W m_{u_i}^2 - 4M_W M_Z s_{\alpha+\beta}s_\beta s_W^2\}U_{s,2}^{\tilde{u},i}U_{t,2}^{\tilde{u},i} + 3c_W m_{u_i}\{A_{ii}^u c_\alpha + (\mu + A_{ii}'^u)s_\alpha\}U_{s,2}^{\tilde{u},i}U_{t,1}^{\tilde{u},i}]. \quad (5)$$

The coupling of the charged Higgs boson H^- to up-type and down-type squarks is given by

$$C(H^-,\tilde{u}_i^s,\tilde{d}_j^t) = \frac{ieV_{ij}^{\rm CKM}}{2M_W s_W s_\beta}[m_{u_i}U_{s,2}^{\tilde{u},i}U_{t,1}^{\tilde{d},j}\{A_{ii}^u + (\mu + A_{ii}'^u)t_\beta\}$$
$$+ m_{u_i}m_{d_j}U_{s,2}^{\tilde{u},i}U_{t,2}^{\tilde{d},j}(1+t_\beta^2)$$
$$+ U_{s,1}^{\tilde{u},i}U_{t,2}^{\tilde{d},j}mt_\beta\{A_{ii}^d t_\beta + (\mu + A_{ii}'^d)\}$$
$$+ U_{s,1}^{\tilde{u},i}U_{t,1}^{\tilde{d},j}\{m_{u_i}^2 - t_\beta(M_W^2 s_{2\beta} - m_{d_j}^2)t_\beta\}]. \quad (6)$$

Here i, j are the generation indices (we assume flavor conservation throughout the paper), $U_{s,s'}^{\tilde{u},i}$ ($U_{t,t'}^{\tilde{d},j}$) is the 2×2 rotation matrix for up-type (down-type) squarks and we use the shorthand notation s_x, c_x, t_x for $\sin x$, $\cos x$, $\tan x$, respectively, where α is the CP-even Higgs mixing angle. The couplings of the heavy CP-even Higgs boson H to the up-type squarks can be obtained by replacing $c_\alpha \to s_\alpha$, $s_\alpha \to -c_\alpha$ and $s_{\alpha+\beta} \to -c_{\alpha+\beta}$ in Eq. (5). It is interesting to observe that A'_t enters differently into the scalar top masses and the trilinear Higgs-stop couplings. This will be crucial for our numerical analysis, see the discussion in Sec. IV.

III. HIGHER-ORDER CORRECTIONS IN THE NHSSM HIGGS SECTOR

A. Tree-level structure and higher-order corrections

The MSSM (and thus the NHSSM) Higgs-boson sector consists of two Higgs doublets and predicts the existence of five physical Higgs bosons, the light and heavy CP-even h and H, the CP-odd A, and a pair of charged Higgs bosons, $H^\pm$. At the tree level the Higgs sector is described with the help of two parameters; the mass of the A boson, M_A, and $\tan\beta$. The tree-level relations and in particular the tree-level masses receive large higher-order corrections, see, e.g., Refs. [8,32,33] and references therein.

The lightest MSSM Higgs boson, with the mass M_h, can be interpreted as the new state discovered at the LHC around ∼125 GeV [34]. The present experimental uncertainty at the LHC for M_h, is about [5],

$$\delta M_h^{\rm exp,today} \sim 140\ {\rm MeV}. \quad (7)$$

This can possibly be reduced below the level of

$$\delta M_h^{\rm exp,future} \lesssim 50\ {\rm MeV} \quad (8)$$

at future e^+e^- colliders [35]. Similarly, for the masses of the heavy neutral Higgs M_H, an uncertainty at the 1% level could be expected at the LHC [36].

In the Feynman diagrammatic (FD) approach that we are following in our calculation here, the higher-order corrected CP-even Higgs boson masses are obtained by finding the poles of the (h,H)-propagator matrix. The inverse of this matrix is given by

$$(\Delta_{\rm Higgs})^{-1} = -i\begin{pmatrix} p^2 - m_{H,\rm tree}^2 + \hat{\Sigma}_{HH}(p^2) & \hat{\Sigma}_{hH}(p^2) \\ \hat{\Sigma}_{hH}(p^2) & p^2 - m_{h,\rm tree}^2 + \hat{\Sigma}_{hh}(p^2) \end{pmatrix}. \quad (9)$$

Determining the poles of the matrix $\Delta_{\rm Higgs}$ in Eq. (9) is equivalent to solving the equation

$$[p^2 - m_{h,\rm tree}^2 + \hat{\Sigma}_{hh}(p^2)][p^2 - m_{H,\rm tree}^2 + \hat{\Sigma}_{HH}(p^2)] - [\hat{\Sigma}_{hH}(p^2)]^2 = 0. \quad (10)$$

Similarly, in the case of the charged Higgs sector, the corrected Higgs mass is derived by the position of the pole in the charged Higgs propagator (for details see Ref. [37] and references therein), which is defined by

$$p^2 - m^2_{H^\pm,\text{tree}} + \hat{\Sigma}_{H^-H^+}(p^2) = 0. \tag{11}$$

The (renormalized) Higgs-boson self-energies in Eqs. (10) and (11) can be evaluated at the n-loop level by an explicit (FD) calculation of the corresponding loop diagrams. As discussed above, in this work we will concentrate on the one-loop corrections from the top/stop sector. The FD contributions to the Higgs-boson self-energies can be supplemented by a resummation of leading and subleading logarithmic contributions, which are relevant in the case of heavy scalar tops. For more details, see Ref. [8]. This will be relevant for the numerical evaluation presented below in Sec. IV.

B. Nonholomorphic contributions to Higgs sector

The NH soft SUSY-breaking parameters enter into the one-loop prediction of the various (renormalized) Higgs-boson self-energies and tadpoles. As discussed above, they can enter into the scalar fermion masses, where, however, their effect can be compensated by a change in the corresponding holomorphic trilinear coupling. They also enter into the Higgs-sfermion-sfermion coupling, see Eq. (5), which will have the main effect in our analysis. Generic Feynman diagrams that involve NH couplings are shown in Fig. 1. Here we restrict ourselves to quark/squark contributions only.

In the following, we briefly describe our workflow for the calculation. To calculate the NH contributions to the Higgs-boson self-energies, we first created an NHSSM model file for FeynArts using *Mathematica* package SARAH [38–42]. The FeynArts/FormCalc [19–22] packages have then been used to analytically calculate the NHSSM contributions to the Higgs-boson self-energies, given as a function of A_t and A'_t. For the numerical evaluation with the FeynArts/FormCalc setup the FormCalc driver files had to be adjusted from the MSSM to the NHSSM. Concerning the numerical evaluation, for a given value of A_t^{MSSM} in the MSSM and A'_t in the NHSSM a new value of A_t^{NHSSM} is calculated such that $X_t^{\text{MSSM}} = A_t^{\text{MSSM}} - \mu\cot\beta$ and $X_t^{\text{NHSSM}} = A_t^{\text{NHSSM}} - (\mu + A'_t)\cot\beta$ are identical (yielding the same values for the stop masses and mixing, see the discussion in the next section). Using A_t^{NHSSM} and A'_t the NH contribution to the Higgs-boson self-energies is calculated numerically. To avoid double counting, we subtracted the Higgs-boson self-energy values at $A'_t = 0$ (i.e. $A_t^{\text{MSSM}} \equiv A_t^{\text{NHSSM}}$) from the obtained results.

These numerical values were fed to FeynHiggs [23–25, 27–30,43] using the FeynHiggs function `FHAddSelf` (where in FeynHiggs the value A_t^{MSSM} was used). The FeynHiggs package already contains the complete set of one-loop corrections in the MSSM. Those are supplemented with leading and subleading two-loop corrections as well as a resummation of leading and subleading logarithmic contributions from the $t/\tilde{t}$ sector. In this way, we include the NH contributions from A'_t into the most precise evaluation of the MSSM Higgs-boson masses available. This allows us to readily estimate the effect of the NH soft SUSY-breaking terms.

IV. NUMERICAL RESULTS

A. General strategy

The leading corrections to M_h from the top/scalar top loops in the NHSSM have been calculated in Ref. [17] and are given by

$$\Delta m^2_{h,t/\tilde{t}} = \frac{3g_2^2 m_t^4}{8\pi^2 M_W^2}\left[\ln\left(\frac{m_{\tilde{t}_1} m_{\tilde{t}_2}}{m_t^2}\right) + \frac{X_t^2}{m_{\tilde{t}_1} m_{\tilde{t}_2}}\left(1 - \frac{X_t^2}{12 m_{\tilde{t}_1} m_{\tilde{t}_2}}\right)\right], \tag{12}$$

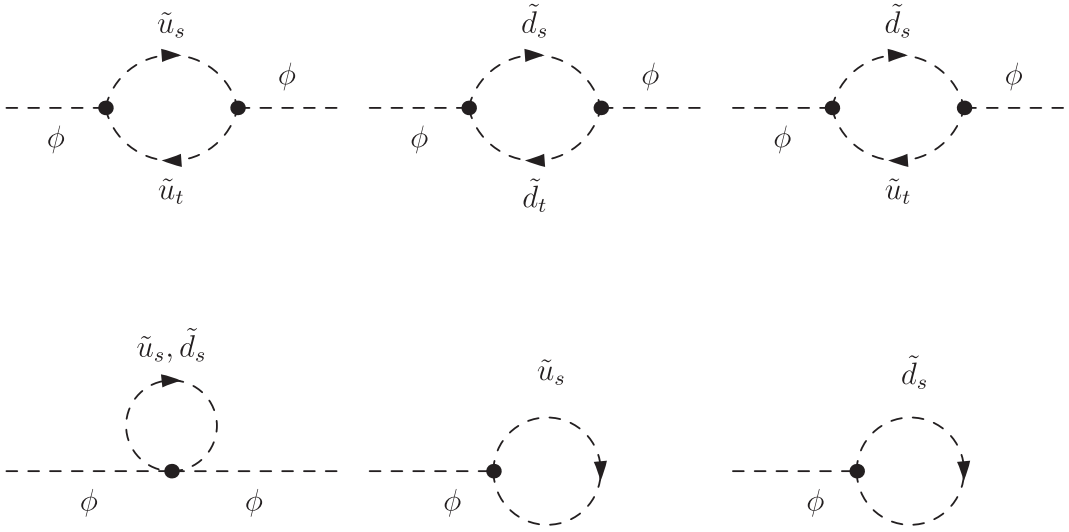

FIG. 1. Generic Feynman diagrams for the Higgs boson self-energies and tadpoles. ϕ denotes any of the Higgs bosons, h, H, A or $H^\pm$; u stands for u, c, t; d stands for d, s, b; $\tilde{u}_{s,t}$ and $\tilde{d}_{s,t}$ are the six mass eigenstates of up-type and down-type squarks, respectively.

where $X_t^{\mathrm{NHSSM}} =: X_t = A_t - (\mu + A_t')\cot\beta$. The nonholomorphic trilinear coupling A_t' affects the X_t parameter as well as the scalar top-quark masses and mixing angle. A simple change in the value of A_t' with fixed A_t will result in the change of X_t which in turn will change M_h. However, with this approach, we can not identify the pure NHSSM contribution, as the same results can be obtained by a correspondingly changed value of A_t in the MSSM. Moreover, (if SUSY is realized in nature) the scalar top masses and mixing will be known in the future and the choice of the soft SUSY-breaking parameters have to reproduce their values. Therefore it makes sense to analyze the NH effects in a scheme that allows keeping the two stop masses and the mixing angle fixed. On the other hand, in the FD approach A_t' appears also in the coupling of the Higgs boson to the scalar top quarks. In order to estimate the contributions to the Higgs-boson mass spectrum coming purely from A_t', it is therefore important to fix the value of the parameter X_t (see the discussion in the previous section), shifting the NH effects completely into the change in the Higgs-stop coupling.

B. Benchmark scenarios

In our numerical analyses, we have followed the above-described approach. We evaluated the results in three benchmark scenarios defined in Ref. [44] that are used by the ATLAS and CMS Collaboration for their interpretation of MSSM Higgs boson searches. These are the M_h^{125} scenario (heavy SUSY particles, effectively the two-Higgs doublet model type-II with SUSY restrictions on Higgs-boson masses and couplings), the $M_h^{125}(\tilde{\tau})$ scenario (featuring light scalar taus) and the $M_h(\tilde{\chi})$ scenario (featuring light charginos and neutralinos). The three scenarios are compatible with the LHC searches for SUSY particles and yield a light CP-even Higgs boson with a mass around 125 GeV with SM-like properties. For these scenarios indirect constraints like dark matter density, flavor observables, and the anomalous magnetic moment of the muon on the MSSM parameters space are not taken into account on purpose [44]. These potential constraints mainly depend on the parameters that are not important for the Higgs-boson phenomenology. Alternatively, small variations in the MSSM can invalidate this type of constraints, while leaving the Higgs-boson phenomenology largely unaffected, see the discussion in Ref. [44]. We furthermore assume that there is no (relevant) flavor violation. Consequently, the first and second generation scalar fermions have a very mild effect on the predictions of the Higgs masses and mixing. Thus, a common soft SUSY-breaking mass $M_{\tilde{f}} = 2$ TeV and corresponding Higgs-sfermion interaction terms $A_f = 0$ are assumed for first- and second-generation sfermions in the benchmark scenarios. This is in full agreement with the current exclusion bounds from CMS [45] and ATLAS [46,47]. In Table I, we list the remaining soft SUSY-breaking input parameters with their corresponding scalar top masses for the three scenarios considered in our numerical analysis.

TABLE I. Selected scenarios in the MSSM parameter space, taken from Ref. [44].

	M_h^{125}	$M_h^{125}(\tilde{\tau})$	$M_h^{125}(\tilde{\chi})$
$m_{\tilde{Q}_3,\tilde{U}_3,\tilde{D}_3}$	1.5 TeV	1.5 TeV	1.5 TeV
$m_{\tilde{L}_3,\tilde{E}_3}$	2 TeV	350 GeV	2 TeV
μ	1 TeV	1 TeV	180 GeV
M_1 a	1 TeV	180 GeV	160 GeV
M_2	1 TeV	300 GeV	180 GeV
M_3	2.5 TeV	2.5 TeV	2.5 TeV
X_t	2.8 TeV	2.8 TeV	2.5 TeV
A_τ	0	800 GeV	0
A_b	0	0	0
$m_{\tilde{t}_1}, m_{\tilde{t}_2}$	1339, 1662 GeV	1339, 1662 GeV	1358, 1646 GeV

For each scenario, we investigate three different combinations of M_A and $\tan\beta$, taking into account the latest experimental limits for MSSM Higgs-boson searches [45,46]:

(i) P1: $M_A = 1000$ GeV, $\tan\beta = 7$,
(ii) P2: $M_A = 1500$ GeV, $\tan\beta = 15$, and
(iii) P3: $M_A = 2000$ GeV, $\tan\beta = 45$.

For our numerical analysis, the values of A_t and A_t' have been chosen such that the value of X_t remains constant as given in the three scenarios in Table I. However, in order to extract pure NHSSM contributions we treat A_b and A_τ independent from A_t (contrary to the definition in Ref. [44]) and concentrate only on the top/stop sector. Here it should be noted that the bottom/sbottom and tau/stau contributions can also result in large radiative corrections to the renormalized Higgs-boson self-energies due to the fact that the corresponding nonholomorphic trilinear couplings A_b' and A_τ' are multiplied by $\tan\beta$. However, a fixed value of $X_b(X_\tau)$, as our strategy requires, can result in an unrealistically large value of $A_b(A_\tau)$. Furthermore, this can lead to severe numerical instabilities in the evaluation of the Higgs-boson spectra, even for moderate values of A_b' and A_τ', and special care has to be taken to remain in a perturbative and numerically-stable regime of the model. Consequently, here we restrict ourselves to the corrections from the top/stop sector (as it had been done in Ref. [17]), allowing us to pin down the NH effects. We leave a corresponding analysis of the effects of A_b' and A_τ' for future work.

C. NH contributions to renormalized Higgs-boson self-energies

In this subsection, we present our results for the NH effects on the renormalized Higgs-boson self-energies in the scenarios defined in the previous subsection. To highlight the nonholomorphic contributions, we define

$$\delta\hat{\Sigma}_{hh} = \hat{\Sigma}_{hh} - \hat{\Sigma}^{\rm MSSM}_{hh},$$
$$\delta\hat{\Sigma}_{hH} = \hat{\Sigma}_{hH} - \hat{\Sigma}^{\rm MSSM}_{hH},$$
$$\delta\hat{\Sigma}_{HH} = \hat{\Sigma}_{HH} - \hat{\Sigma}^{\rm MSSM}_{HH},$$
$$\delta\hat{\Sigma}_{H^\pm} = \hat{\Sigma}_{H^\pm} - \hat{\Sigma}^{\rm MSSM}_{H^\pm}, \tag{13}$$

and

$$\delta M_h = M_h - M_h^{\rm MSSM},$$
$$\delta M_H = M_H - M_H^{\rm MSSM},$$
$$\delta M_{H^\pm} = M_{H^\pm} - M_{H^\pm}^{\rm MSSM}, \tag{14}$$

where $\hat{\Sigma}^{\rm MSSM}_{hh}$, $\hat{\Sigma}^{\rm MSSM}_{hH}$, $\hat{\Sigma}^{\rm MSSM}_{HH}$, $\hat{\Sigma}^{\rm MSSM}_{H^\pm}$, $M_h^{\rm MSSM}$, $M_H^{\rm MSSM}$, and $M_{H^\pm}^{\rm MSSM}$ corresponds to the renormalized Higgs-boson self-energies and Higgs-boson masses with $A_t' = 0$.

The contributions of the nonholomorphic trilinear coupling A_t' to the renormalized Higgs boson self energies, $\delta\hat{\Sigma}_{hh}$, $\delta\hat{\Sigma}_{hH}$, $\delta\hat{\Sigma}_{HH}$, and $\delta\hat{\Sigma}_{H^\pm}$ are shown as a function of A_t' in Figs. 2–5, respectively. We have varied A_t' in the interval -3000 GeV to $+3000$ GeV. In each figure, we show in the left (right) plot the results for the M_h^{125} ($M_h^{125}(\tilde{\chi})$) scenario for P1 (P2, P3) in blue (orange, violet) dashed lines. The results in the $M_h^{125}(\tilde{\tau})$ scenario are effectively identical to the ones obtained in the M_h^{125} scenario, as could be expected from the identical parameter values in the scalar top sector. Consequently, we refrain from showing them separately. On the other hand, as can be seen from these figures the results for the renormalized Higgs-boson self-energies differ slightly between M_h^{125}, $M_h^{125}(\tilde{\tau})$, and $M_h^{125}(\tilde{\chi})$. This can be traced back to the different A_t values found in the three scenarios, which in turn stem from the different baseline values of X_t and in particular of μ in M_h^{125}, $M_h^{125}(\tilde{\tau})$ with respect to $M_h^{125}(\tilde{\chi})$. As an example, for $\tan\beta = 45$ we find an interval of $A_t^{\rm NHSSM} = 2755$ GeV to 2888 GeV for the first two benchmarks, whereas $A_t^{\rm NHSSM} = 2437$ GeV to 2570 GeV is found in the latter.

For the renormalized self-energies of the neutral CP-even Higgs bosons we observe as a general order of magnitude for the absolute values of the corrections that $\delta\hat{\Sigma}_{hh} < \delta\hat{\Sigma}_{hH} < \delta\hat{\Sigma}_{HH} \sim \delta\hat{\Sigma}_{H^\pm}$. This can be understood from the fact that the new NH soft SUSY-breaking term

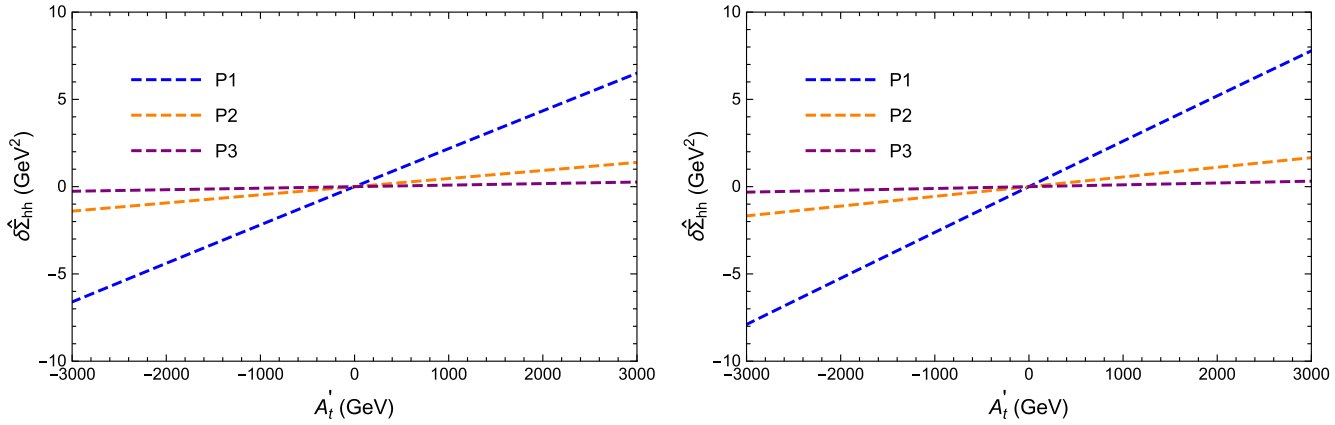

FIG. 2. $\delta\hat{\Sigma}_{hh}$ as a function of A_t' for M_h^{125} (left) and $M_h^{125}(\tilde{\chi})$ (right plot). The results in $M_h^{125}(\tilde{\tau})$ are effectively identical to M_h^{125} and consequently not shown.

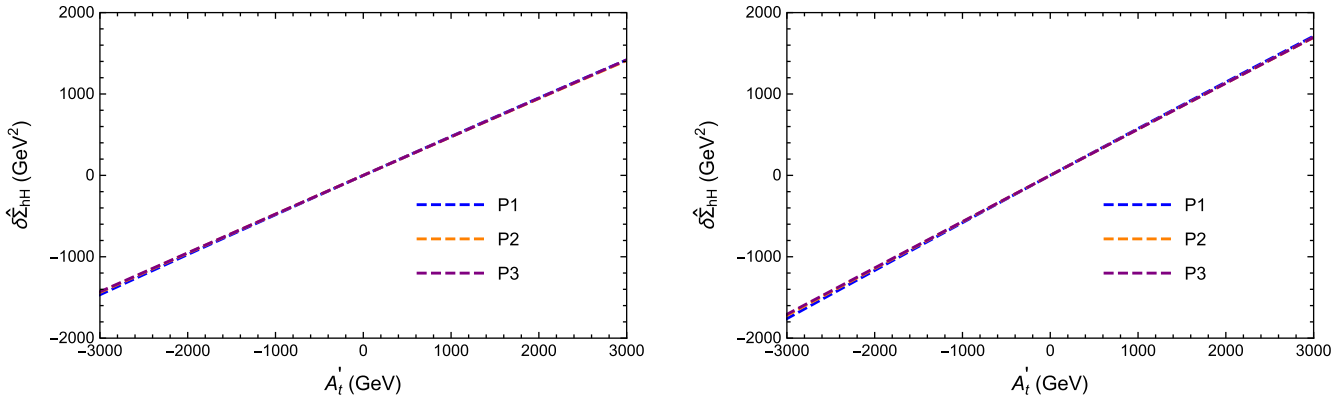

FIG. 3. $\delta\hat{\Sigma}_{hH}$ as a function of A_t' for M_h^{125} (left) and $M_h^{125}(\tilde{\chi})$ (right plot).

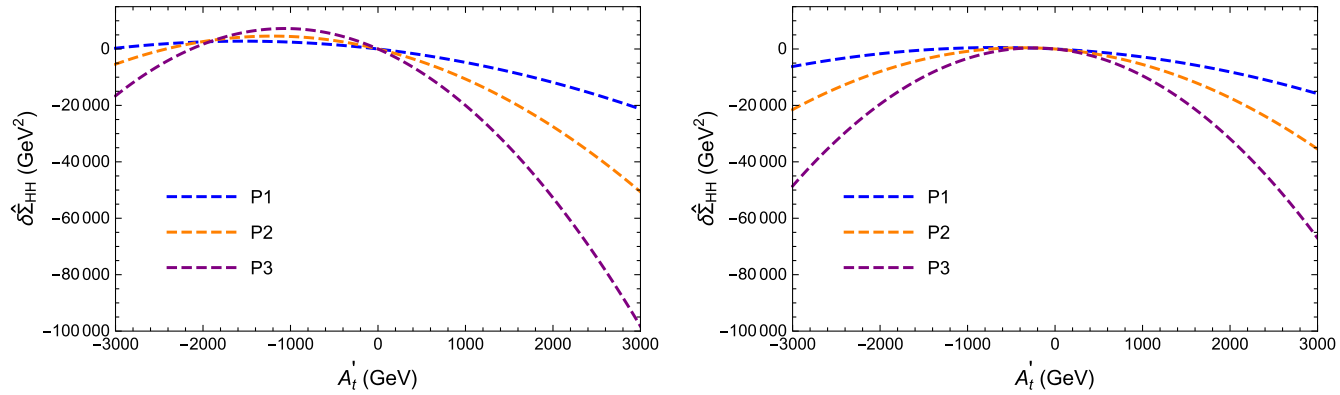

FIG. 4. $\delta\hat{\Sigma}_{HH}$ as a function of A_t' for M_h^{125} (left) and $M_h^{125}(\tilde{\chi})$ (right plot).

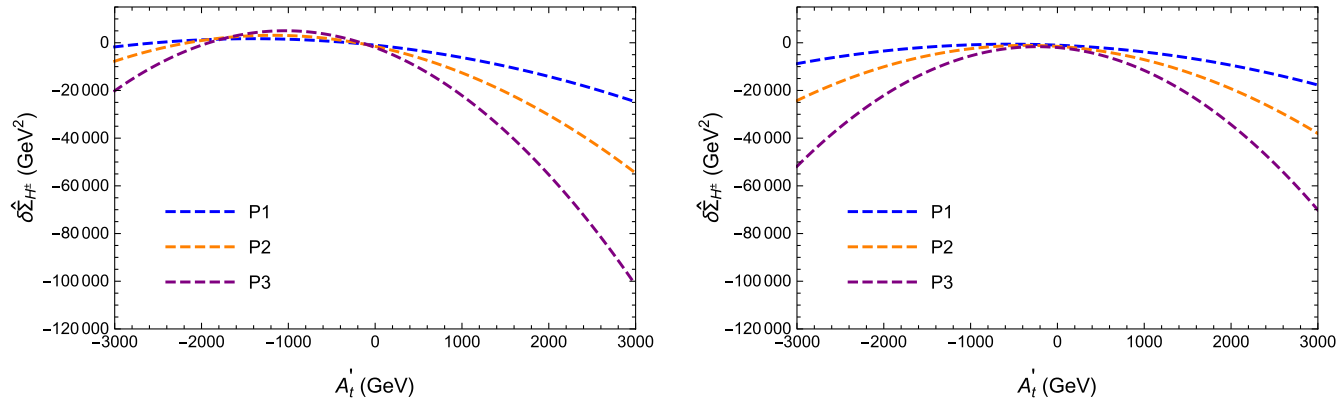

FIG. 5. $\delta\hat{\Sigma}_{H^\pm}$ as a function of A_t' for M_h^{125} (left) and $M_h^{125}(\tilde{\chi})$ (right plot).

A_t' pairs preferably with the first Higgs doublet, see Eq. (2). The light CP-even Higgs, h, has a large contribution from the second Higgs doublet, whereas the H has a large part from the first Higgs doublet. Consequently, the largest effects are expected in the coupling of the heavy CP-even Higgs to scalar tops. The largest effects on $\hat{\Sigma}_{hh}$ are found in P1 with $\sim \mp 7\text{GeV}^2$ for $A_t' = \mp 3000\text{GeV}$, respectively, with only a small variation between the three benchmark scenarios. The effect increases to $\mp 1500\text{GeV}^2$ for $\hat{\Sigma}_{hH}$, nearly equal for all benchmarks and points. The largest effects are found for $\hat{\Sigma}_{HH}$, reaching up to $\sim -100000\ \text{GeV}^2$ for P3 in the M_h^{125} and $M_h^{125}(\tilde{\tau})$ scenario for $A_t' = 3000$ GeV, and up to $\sim -70000\ \text{GeV}^2$ for P3 in the $M_h^{125}(\tilde{\chi})$. For $\hat{\Sigma}_{HH}$ a strong variation between the three M_A-$\tan\beta$ combinations can be observed, where larger M_A values, which in turn allow for larger $\tan\beta$ lead to the most sizable effects. This can be understood from the corresponding $\tan\beta$ enhancement of the A_t' contribution. Very similar effects can be observed for the renormalized charged Higgs-boson self-energy, as shown in Fig. 5. Also for the charged Higgs-boson, residing largely in the first Higgs doublet, the A_t' coupling contribution is enhanced with $\tan\beta$, see Eq. (6).

D. NH contributions to the Higgs-boson masses

We now turn to the numerical evaluation of the impact of the NH trilinear coupling A_t' on the higher-order corrected Higgs-boson masses themselves. The results shown in the previous subsection were obtained by subtracting the Higgs-boson self-energies values at $A_t' = 0$, i.e. the pure MSSM contribution. This allows us to directly add these new contributions to the full calculation of the renormalized Higgs-boson self-energies in the MSSM. In order to estimate their effects on the Higgs-bosons masses, we fed these results to the code FeynHiggs using the FeynHiggs function `FHAddSelf`. This function adds the NHSSM contributions to the renormalized Higgs boson self-energies in the MSSM evaluated at the highest level of precision. For details see the discussion at the end of Sec. III B and in Sec. IV A.

The obtained results are shown as a function of A_t' in Figs. 6–8 for δM_h, δM_H, and $\delta M_{H^\pm}$, respectively. As in the

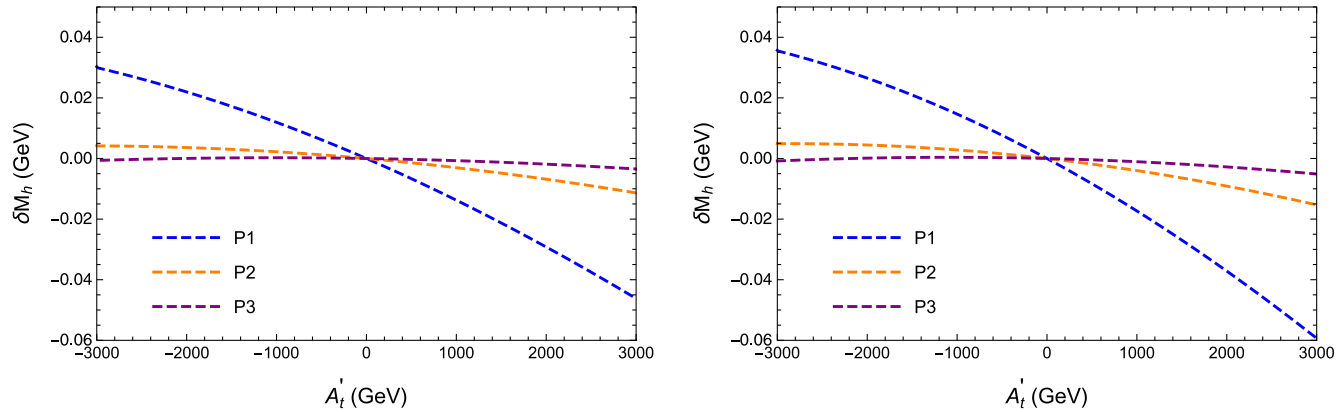

FIG. 6. δM_h as a function of A_t' for M_h^{125} (left) and $M_h^{125}(\tilde{\chi})$ (right plot). The results in $M_h^{125}(\tilde{\tau})$ are effectively identical to M_h^{125} and consequently not shown.

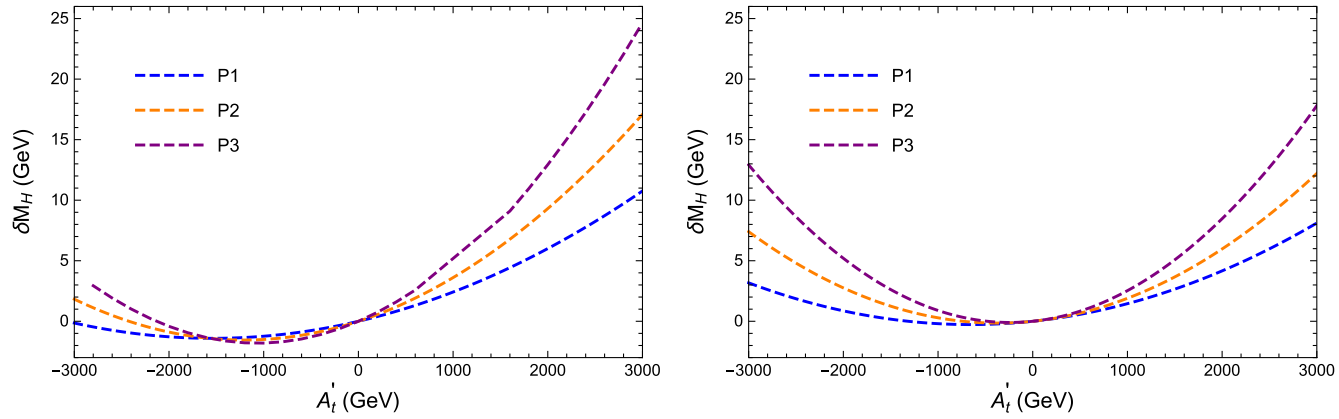

FIG. 7. δM_H as a function of A_t' for M_h^{125} (left), and $M_h^{125}(\tilde{\chi})$ (right plot).

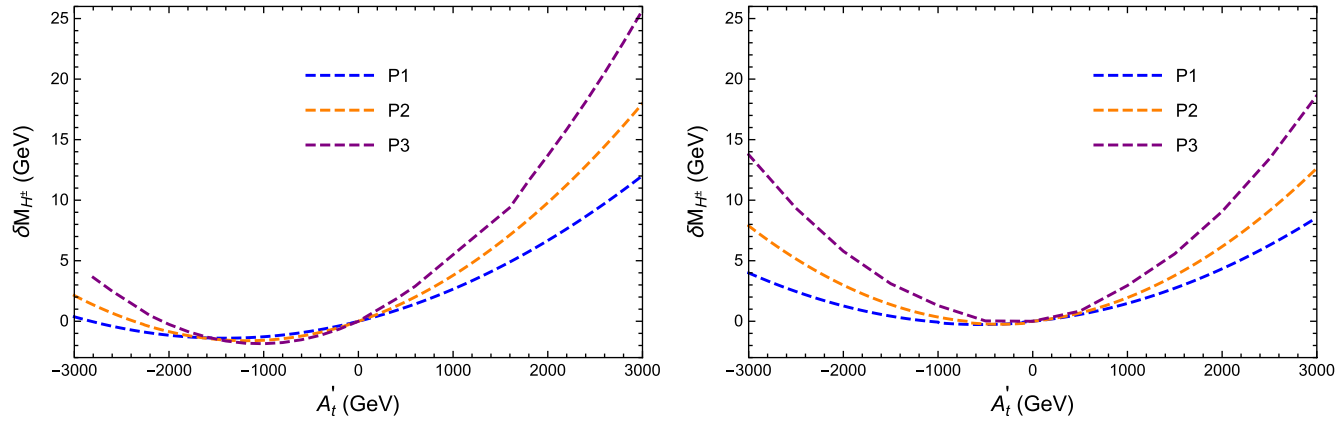

FIG. 8. $\delta M_{H^\pm}$ as a function of A_t' for M_h^{125} (left) and $M_h^{125}(\tilde{\chi})$ (right plot).

previous subsection, we use the interval of $A_t' = -3000$ GeV to $+3000$ GeV. The order of the plots and the color coding are as in the previous subsection. In particular, we again do not show the results for $M_h^{125}(\tilde{\tau})$, as they are effectively identical to the ones in the M_h^{125} scenario. Since the absolute effects on the renormalized Higgs-boson self-energies follow the pattern $\delta\hat{\Sigma}_{hh} < \delta\hat{\Sigma}_{hH} < \delta\hat{\Sigma}_{HH} \sim \delta\hat{\Sigma}_{H^\pm}$, one expects larger effects for the two heavy Higgs-boson masses than for the light CP-even Higgs. Only for very large values of $M_A^2 \gg |\delta\hat{\Sigma}_{HH}|, |\delta\hat{\Sigma}_{H^\pm}|$

the additional contributions from NH terms should become irrelevant for M_H and $M_{H^\pm}$.

For δM_h, as shown in Fig. 6, the NH contributions yield corrections that in general are found to be very small, as could be expected from the size of $\delta\hat{\Sigma}_{hh}$, see Fig. 2. They reach up to ~ -45 MeV for $A_t' = 3000$ GeV in the M_h^{125} and $M_h^{125}(\tilde{\tau})$ scenario for P1, with negligible changes in P2 and P3. In these two benchmark scenarios, the corrections for negative A_t' stay below $+30$ MeV. In the $M_h^{125}(\tilde{\chi})$ scenario the results look similar, with slightly larger corrections in P1. The fact that P1 exhibits the largest corrections corroborates that this effect on M_h, as expected, stems from the contribution of $\delta\hat{\Sigma}_{hh}$. The fact that the corrections turn out to be very small over the whole analyzed parameter space demonstrates that the NH terms *do not* alleviate the finding that large stop masses are needed to reach the value of $M_h \sim 125$ GeV. On the other hand, the effects from A_b' and/or A_τ' could show a different behavior. We leave this analysis for future work. It should be noted here that the size of the numerical effects on M_h found here are substantially smaller than previously claimed in the literature [17]. This can be explained by the fact that we ensured to compare results including the NH effects to the "pure MSSM", but leaving the physics scenario (the stop masses and mixing) unchanged.

The changes in the heavy CP-even Higgs-boson mass, M_H, are shown in Fig. 7. The general pattern follows the size of the corrections for $\delta\hat{\Sigma}_{HH}$, as shown in Fig. 4. Contrary to M_h, for M_H the corrections turn out to be in general positive. The largest values reached are $\sim +25$ GeV for $A_t' = 3000$ GeV in P3 in the M_h^{125} and the $M_h^{125}(\tilde{\tau})$ scenario. In the $M_h^{125}(\tilde{\chi})$ scenario the largest corresponding value is $\sim +18$ GeV. For $A_t' = -3000$ GeV the corrections reach up to $+5$ GeV in P3 for the first two benchmarks, and up to $+13$ GeV for the third, with correspondingly smaller values for P2 and P1.

As a last step, we show the changes in the charged Higgs-boson mass, $M_{H^\pm}$, in Fig. 8. As can be expected from the NH contributions to the renormalized Higgs-boson self-energies, which are similar for $\delta\hat{\Sigma}_{HH}$ and $\delta\hat{\Sigma}_{H^\pm}$, see Figs. 4 and 5, also the correction to the two heavy Higgs-boson masses themselves turn out to be similar. $\delta M_{H^\pm}$ follows in sign and size the corrections found for M_H. The NH contributions *do not* lead to an enhanced splitting between the M_H and $M_{H^\pm}$, but only to larger differences between M_A (our input) and the other two heavy Higgs-boson masses.

V. CONCLUSIONS

In this paper, we have investigated the effect of nonholomorphic soft SUSY-breaking terms to the Higgs-boson mass predictions in the MSSM, a model dubbed NHSSM. In order to perform the calculations we generated the FeynArts model file using the *Mathematica* package SARAH. The model file was then used in the FeynArts/FormCalc setup (including modifications in the FormCalc driver files to adapt the NHSSM specific input) to generate analytical and numerical results for the various renormalized Higgs boson self-energies. We concentrated on the contributions from the top/scalar top sector. The relevant NH term is the trilinear coupling A_t'. The results for the renormalized Higgs-boson self-energies were then fed into the code FeynHiggs (using the `FHAddSelf` subroutine) to calculate the predictions for the Higgs-boson masses.

We took particular care to analyze the pure NH contribution. The A_t' contributions enter into the scalar top mass matrix via the nondiagonal entry X_t, as well as into the Higgs-stop couplings. An analysis simply varying A_t' thus leads to a shift in the scalar top masses, which should be considered as a different physics scenario, since the stop masses and mixing angle are expected to be measured in the future (if SUSY is realized). Consequently, an observed effect from a naive variation of A_t' can be mimicked by a change in the holomorphic soft SUSY-breaking terms, in particular the trilinear Higgs-stop coupling, A_t; for each choice of A_t' the parameter A_t can be adjusted to yield the same scalar top mass. An observed scalar top mass spectrum thus corresponds to a continuous set of combinations of A_t and A_t' (keeping the other soft SUSY-breaking parameters and μ fixed). An analysis that simply varies A_t', resulting in shifts in the scalar top masses, can thus not be regarded realistic. Therefore, in our analysis, we required X_t to be constant under a change of A_t' by an adjustment of A_t. In this way, the effect of the NH contributions is shifted into the Higgs-stop couplings and can readily be analyzed.

For the NH contributions to the renormalized Higgs-boson self-energies we find (in absolute terms) $\delta\hat{\Sigma}_{hh} < \delta\hat{\Sigma}_{hH} < \delta\hat{\Sigma}_{HH} \sim \delta\hat{\Sigma}_{H^\pm}$. This can be understood from the fact that the new NH soft SUSY-breaking term A_t' pairs preferably with the first Higgs doublet. The light CP-even Higgs, h, has a large contribution from the second Higgs doublet, whereas the H, as well as the charged Higgs have their largest component from the first Higgs doublet. Consequently, the largest effects are expected in the coupling of the heavy CP-even Higgs, or the charged Higgs to scalar tops.

For the numerical analysis, we chose three LHC benchmark scenarios [M_h^{125}, $M_h^{125}(\tilde{\tau})$, and $M_h^{125}(\tilde{\chi})$], and in each scenario, three combinations of $(M_A, \tan\beta)$ that are allowed by current MSSM Higgs-boson searches at the LHC, (1000 GeV, 7), (1500 GeV, 15), (2000 GeV, 45), called P1, P2, P3, respectively. A_t' has been varied from -3000 GeV to $+3000$ GeV. The results in the M_h^{125} and the $M_h^{125}(\tilde{\tau})$ scenario, are effectively identical due to their identical settings in the scalar top sector. The results in the $M_h^{125}(\tilde{\chi})$ scenario, however, can vary substantially from the other two scenarios. For δM_h the NH contributions yield corrections that are in general found to be very small, contrary to previous claims in the literature. They reach up

to ~ -60 MeV in the analyzed parameter space, where P1 exhibits the largest corrections. Since the corrections turn out to be very small over the whole analyzed parameter space we find that the NH terms *do not* alleviate the fact that large stop masses are needed to reach the value of $M_h \sim 125$ GeV. The situation might change for the corrections involving A_b' and/or A_τ', which we leave for future work. The numerical effects for M_H and $M_{H^\pm}$ were found to be in general positive and reached values of up to $+25$ GeV for M_H and $M_{H^\pm}$.

Despite the fact that the NH contributions entering via A_t' are small for M_h, a full analysis of supersymmetric extensions of the SM should include the possibility of NH contributions. We aim for an inclusion of these effects into the code FeynHiggs.

ACKNOWLEDGMENTS

We thank F. Staub for helpful discussions on SARAH and the model file generation for FeynArts. The work of S. H. has received financial support from the Grant No. PID2019–110058GB-C21 funded by MCIN/AEI/10.13039/501100011033 and by "ERDF A way of making Europe" and in part by the IFT Centro de Excelencia Severo Ochoa Grant No. CEX2020-001007-S funded by MCIN/AEI/10.13039/501100011033.

[1] G. Aad *et al.* (ATLAS Collaboration), Phys. Lett. B **716**, 1 (2012).
[2] S. Chatrchyan *et al.* (CMS Collaboration), Phys. Lett. B **716**, 30 (2012).
[3] S. Sekmen (ATLAS, CMS, and LHCb Collaborations), arXiv:2204.03053.
[4] P. Fayet, Nucl. Phys. **B90**, 104 (1975); Phys. Lett. **64B**, 159 (1976); **69B**, 489 (1977); H. Nilles, Phys. Rep. **110**, 1 (1984); H. Haber and G. Kane, Phys. Rep. **117**, 75 (1985); R. Barbieri, Riv. Nuovo Cimento **11**, 1 (1988).
[5] A. M. Sirunyan *et al.* (CMS Collaboration), Phys. Lett. B **805**, 135425 (2020).
[6] M. Arana-Catania, S. Heinemeyer, M. J. Herrero, and S. Penaranda, J. High Energy Phys. 05 (2012) 015.
[7] M. E. Gómez, T. Hahn, S. Heinemeyer, and M. Rehman, Phys. Rev. D **90**, 074016 (2014).
[8] P. Slavich, S. Heinemeyer, E. Bagnaschi, H. Bahl, M. Goodsell, H. E. Haber, T. Hahn, R. Harlander, W. Hollik, G. Lee *et al.*, Eur. Phys. J. C **81**, 450 (2021).
[9] L. Girardello and M. T. Grisaru, Nucl. Phys. **B194**, 65 (1982).
[10] J. Bagger and E. Poppitz, Phys. Rev. Lett. **71**, 2380 (1993).
[11] I. Jack and D. Jones, Phys. Lett. B **457**, 101 (1999).
[12] I. Jack and D. Jones, Phys. Rev. D **61**, 095002 (2000).
[13] I. Jack, D. Jones, and A. Kord, Phys. Lett. B **588**, 127 (2004).
[14] M. Cakir, S. Mutlu, and L. Solmaz, Phys. Rev. D **71**, 115005 (2005).
[15] A. Sabanci, A. Hayreter, and L. Solmaz, Phys. Lett. B **661**, 154 (2008).
[16] C. S. Ün, Ş. H. Tanyıldızı, S. Kerman, and L. Solmaz, Phys. Rev. D **91**, 105033 (2015).
[17] U. Chattopadhyay and A. Dey, J. High Energy Phys. 10 (2016) 027.
[18] U. Chattopadhyay, D. Das, and S. Mukherjee, J. High Energy Phys. 01 (2018) 158.
[19] T. Hahn, Comput. Phys. Commun. **140**, 418 (2001).
[20] T. Hahn and C. Schappacher, Comput. Phys. Commun. **143**, 54 (2002).
[21] T. Fritzsche, T. Hahn, S. Heinemeyer, F. von der Pahlen, H. Rzehak, and C. Schappacher, Comput. Phys. Commun. **185**, 1529 (2014).
[22] T. Hahn and M. Perez-Victoria, Comput. Phys. Commun. **118**, 153 (1999).
[23] S. Heinemeyer, W. Hollik, and G. Weiglein, Eur. Phys. J. C **9**, 343 (1999).
[24] G. Degrassi, S. Heinemeyer, W. Hollik, P. Slavich, and G. Weiglein, Eur. Phys. J. C **28**, 133 (2003).
[25] M. Frank, T. Hahn, S. Heinemeyer, W. Hollik, R. Rzehak, and G. Weiglein, J. High Energy Phys. 02 (2007) 047.
[26] M. Frank, T. Hahn, S. Heinemeyer, W. Hollik, H. Rzehak, and G. Weiglein, J. High Energy Phys. 02 (2007) 047.
[27] T. Hahn, S. Heinemeyer, W. Hollik, H. Rzehak, and G. Weiglein, Phys. Rev. Lett. **112**, 141801 (2014).
[28] H. Bahl and W. Hollik, Eur. Phys. J. C **76**, 499 (2016).
[29] H. Bahl, S. Heinemeyer, W. Hollik, and G. Weiglein, Eur. Phys. J. C **78**, 57 (2018).
[30] H. Bahl, T. Hahn, S. Heinemeyer, W. Hollik, S. Paßehr, H. Rzehak, and G. Weiglein, Comput. Phys. Commun. **249**, 107099 (2020).
[31] J. Chakrabortty and S. Roy, Phys. Rev. D **85**, 035014 (2012).
[32] A. Djouadi, Phys. Rep. **459**, 1 (2008); S. Heinemeyer, Int. J. Mod. Phys. A **21**, 2659 (2006).
[33] P. Draper and H. Rzehak, Phys. Rep. **619**, 1 (2016).
[34] S. Heinemeyer, O. Stal, and G. Weiglein, Phys. Lett. B **710**, 201 (2012).
[35] H. Baer *et al.*, arXiv:1306.6352.
[36] S. Gennai, S. Heinemeyer, A. Kalinowski, R. Kinnunen, S. Lehti, A. Nikitenko, and G. Weiglein, Eur. Phys. J. C **52**, 383 (2007).
[37] M. Frank, L. Galeta, T. Hahn, S. Heinemeyer, W. Hollik, H. Rzehak, and G. Weiglein, Phys. Rev. D **88**, 055013 (2013).
[38] F. Staub, Comput. Phys. Commun. **181**, 1077 (2010).

[39] F. Staub, Comput. Phys. Commun. **182**, 808 (2011).
[40] F. Staub, Comput. Phys. Commun. **184**, 1792 (2013).
[41] F. Staub, Comput. Phys. Commun. **185**, 1773 (2014).
[42] F. Staub, Adv. High Energy Phys. **2015**, 840780 (2015).
[43] S. Heinemeyer, W. Hollik, and G. Weiglein, Comput. Phys. Commun. **124**, 76 (2000); T. Hahn, S. Heinemeyer, W. Hollik, H. Rzehak, and G. Weiglein, Comput. Phys. Commun. **180**, 1426 (2009); See www.feynhiggs.de.
[44] E. Bagnaschi, H. Bahl, E. Fuchs, T. Hahn, S. Heinemeyer, S. Liebler, S. Patel, P. Slavich, T. Stefaniak, C. E. Wagner, and G. Weiglein, Eur. Phys. J. C **79**, 617 (2019).
[45] CMS Collaboration, arXiv:2208.02717.
[46] G. Aad *et al.* (ATLAS Collaboration), Phys. Rev. Lett. **125**, 051801 (2020).
[47] G. Aad *et al.* (ATLAS Collaboration), Eur. Phys. J. C **81**, 600 (2021); **81**, 956(E) (2021).